

# Spatial Regulation of *nanos* Is Required for Its Function in Dendrite Morphogenesis

Jillian L. Brechbiel and Elizabeth R. Gavis

## Supplemental Experimental Procedures

### Fly Strains and Genetics

A *GAL4<sup>477</sup>*, *UAS-mCD8::GFP* recombinant chromosome [S1] was used to mark class IV da neurons with *mcd8::GFP* in all experiments. Larvae mutant for *nos* were generated by using the null combination *nos<sup>RC</sup>/Df(3R)Df<sup>43</sup>* [S2] (Figure 1) or the strong hypomorphic combination *nos<sup>RC</sup>/nos<sup>RD</sup>* [S2] (Figure 2). The *smg* mutant phenotype was evaluated by using the null combination *smg<sup>1</sup>/Df(3L)scf<sup>R6</sup>* [S3]. The null allele *glo<sup>162x</sup>* [S4] was recombined with *smg<sup>1</sup>* to generate the *smg<sup>1</sup> glo<sup>162x</sup>* double mutant. The recombination removed an unlinked lethal mutation from the *smg<sup>1</sup>* chromosome, allowing the generation of homozygous *smg<sup>1</sup> glo<sup>162x</sup>* mutant larvae. An *FRT82B glo<sup>162x</sup>* recombinant was generated and used to produce homozygous *glo<sup>162x</sup>* mutant larvae or MARCM clones. For MARCM, *FRT82B glo<sup>162x</sup>* flies were mated to *elav-GAL4*, *UAS-mcd8::GFP*, *hs-FLP*; *FRT82B tubP-GAL80* flies. Embryos were collected for a 2 hr period and then aged for 3 hr at 25°C. Embryos were then heat shocked twice at 37°C, first for 30 min and then for 60 min, with a 30 min period at 25°C in between. Development to larval stages was allowed to proceed at 25°C. GFP-positive clones were identified in wandering third instar larvae. The *UAS-gloRNAi* strain [S5] was obtained from the Vienna *Drosophila* RNAi Center.

### Transgenes and Transgenic Lines

All *nos* transgenes used here are based on the genomic rescue transgene, *gnos* (previously named *gnosb*) [S6]. The *nos* promoter and 5' genomic sequences present in all *nos* transgenes used here, including those generated previously, are sufficient for expression in class IV da neurons, as determined by using a GFP reporter assay [S7]. The *gnos-tub3'UTR* (previously *nos-tub3'UTR* but renamed here to distinguish from *UAS-nos-tub3'UTR*) and *gnosSREs<sup>-</sup>GRH<sup>-</sup>* transgenes have been previously described [S8, S9]. The *gnosSREs<sup>-</sup>* and *gnosGRH<sup>-</sup>* transgenes contain only the two SRE mutations or the GRH mutation IIIA [S10], respectively. The *nos-(ms2)<sub>18</sub>* transgene is identical to the *nos-(ms2)<sub>5</sub>* transgene [S11] except that it contains 18 tandemly repeated MS2 stem loops. The *nosΔLS-(ms2)<sub>18</sub>*, *nos+1-(ms2)<sub>18</sub>*, and *nos+2-(ms2)<sub>18</sub>* transgenes were generated from *pHSXgnos<sup>R</sup>* [S6] by deleting either a 550 bp EcoRI-XmnI fragment, a 450 bp HpaI-XmnI fragment ( $\Delta 10$  in [S12]), or a 365 bp BglII-XmnI fragment, respectively, from the *nos* 3'UTR. A 1.1 Kb EcoRI-HindIII fragment from *pSL-MS2<sub>18</sub>* (K. Forrest and E.R.G., unpublished data) containing 18 tandemly repeated stem-loop binding sites for MCP was then inserted into the BclI site of the *nos* +6 element still present in each plasmid. The *nosΔLS-(ms2)<sub>18</sub>*, *nos+1-(ms2)<sub>18</sub>*, and *nos+2-(ms2)<sub>18</sub>* inserts were removed as NotI fragments and cloned into *pCaSpeR4* [S13]. The *UAS-MCP-RFP* transgene was constructed similarly to the *hsp83-MCP-RFP* transgene [S11, S14], except that the BamHI-HindIII fragment containing *MCP-RFP-tub3'UTR* was end filled with Klenow and inserted into the end-filled XbaI site of *pUAS<sup>t</sup>* [S15]. To generate the *UASp-smg* transgene, a 3 kb fragment beginning 7 bp upstream of the *smg* translation start codon and extending to the first bp after the translation stop codon was synthesized by PCR from a *smg* cDNA template. KpnI and NotI sites were engineered into the 5' and 3' primers, respectively. After digestion with KpnI and NotI, the fragment was inserted into the *pUASp* vector [S16]. The integrity of the *smg* sequence was confirmed by sequencing. Transgenes were introduced into *y w<sup>67c23</sup>* embryos by P element-mediated germline transformation and multiple independent lines were isolated for each.

### Imaging and Quantitation of Dendrite Morphology

Dendrite morphology in late third instar larvae was analyzed by direct fluorescence imaging of semi-intact preparations. This method facilitated the imaging of the large number of larvae necessary to analyze multiple independent lines for each transgene. Third instar larvae were placed in a pool of PBS and the posterior end, including the spiracles, was snipped off with fine scissors (Fine Science Tools). The remainder of the larva was mounted in 90% glycerol with a #1 1/2 coverglass (VWR). For the analysis of early third instar larvae, larval filets were prepared, immunostained, and mounted as previously described [S7], except that 1:10 Roche Western Blocking Reagent:PBS/0.1% Triton X-100 was used for blocking and

primary antibody incubation. Antibodies used: 1:100 rat anti-mcd8 (Caltag Laboratories), 1:1000 Alexa Fluor 488 goat anti-rat (Molecular Probes). Neurons were imaged on a Zeiss LSM510 microscope by using a 40×/1.2W objective. All neurons were imaged at the same settings, with images collected sequentially at various sections and compiled to create Z series projections.

Branching complexity was quantitated in projections of dorsal da neurons by counting the total number of terminal branches as described in [S17] by using a field of  $1 \times 10^6 \mu\text{m}^2$  positioned to maximize coverage of the dendritic tree between adjacent segments. One neuron from either the third or fourth segment was quantitated per larva. This method produced very similar results to quantitation of a field extending from the cell body to the midline. For example, *smg* mutant neurons showed a 21% decrease in terminal branches as compared to wild-type when quantitated by the first method and a 23% decrease by the second method.

### Live Imaging of Particle Movement

Larvae were anesthetized by immersion in 1:5 chloroform:Voltalet oil (H10S), then placed on a microscope slide in a drop of chloroform:Voltalet. Two 22 × 22 cm coverglasses were positioned, one each side of the drop, and a 22 × 50 cm coverglass was placed over the top. In this configuration, the smaller coverglasses act as spacers to prevent the top coverglass from crushing the larva. Neurons were imaged within 20 min of exposure to anesthesia, using a Perkin Elmer spinning disc microscope with a 63×/1.4 N.A. oil immersion objective. Only neurons with wild-type morphology, as determined by using *mCD8::GFP*, were imaged. Particles were tracked manually by using the Velocity software program. Average particle velocities were measured for individual runs of single particles that were visible in at least six consecutive frames of capture (average run time = 8.9 s or 22 frames) and the average of these velocities (mean average velocity) was calculated.

### Supplemental References

- S1. Grueber, W.B., Jan, L.Y., and Jan, Y.N. (2003). Different levels of the homeodomain protein Cut regulate distinct dendrite branching patterns of *Drosophila* multidendritic neurons. *Cell* 112, 805–818.
- S2. Curtis, D., Treiber, D.K., Tao, F., Zamore, P.D., Williamson, J.R., and Lehmann, R. (1997). A CCHC metal-binding domain in Nanos is essential for translational regulation. *EMBO J.* 16, 834–843.
- S3. Dahanukar, A., Walker, J.A., and Wharton, R.P. (1999). Smaug, a novel RNA-binding protein that operates a translational switch in *Drosophila*. *Mol. Cell* 4, 209–218.
- S4. Kalifa, Y., Huang, T., Rosen, L.N., Chatterjee, S., and Gavis, E.R. (2006). Giorund, an hnRNP F/H homolog, is an ovarian repressor of *nanos* translation. *Dev. Cell* 10, 291–301.
- S5. Dietzl, G., Chen, D., Schnorrrer, F., Su, K.C., Barinova, Y., Fellner, M., Gasser, B., Kinsey, K., Oettel, S., Scheiblaue, S., et al. (2007). A genome-wide transgenic RNAi library for conditional gene inactivation in *Drosophila*. *Nature* 448, 151–156.
- S6. Gavis, E.R., and Lehmann, R. (1992). Localization of *nanos* RNA controls embryonic polarity. *Cell* 71, 301–313.
- S7. Ye, B., Petritsch, C., Clark, I.E., Gavis, E.R., Jan, L.Y., and Jan, Y.N. (2004). *nanos* and *pumilio* are essential for dendrite morphogenesis in *Drosophila* peripheral neurons. *Curr. Biol.* 14, 314–321.
- S8. Gavis, E.R., and Lehmann, R. (1994). Translational regulation of *nanos* by RNA localization. *Nature* 369, 315–318.
- S9. Gavis, E.R., Chatterjee, S., Ford, N.R., and Wolff, L.J. (2008). Dispensability of *nanos* mRNA localization for abdominal patterning but not for germ cell development. *Mech. Dev.* 125, 81–90.
- S10. Cruces, S., Chatterjee, S., and Gavis, E.R. (2000). Overlapping but distinct RNA elements control repression and activation of *nanos* translation. *Mol. Cell* 5, 457–467.
- S11. Forrest, K.M., and Gavis, E.R. (2003). Live imaging of endogenous mRNA reveals a diffusion and entrapment mechanism for *nanos* mRNA localization in *Drosophila*. *Curr. Biol.* 13, 1159–1168.
- S12. Gavis, E.R., Curtis, D., and Lehmann, R. (1996). Identification of cis-acting sequences that control *nanos* RNA localization. *Dev. Biol.* 176, 36–50.

- S13. Pirrotta, V. (1988). Vectors for P-mediated transformation in *Drosophila*. *Biotechnology* 10, 437–456.
- S14. Weil, T.T., Forrest, K.M., and Gavis, E.R. (2006). Localization of *bicoid* mRNA in late oocytes is maintained by continual active transport. *Dev. Cell* 11, 251–262.
- S15. Brand, A.H., and Perrimon, N. (1993). Targeted gene expression as a means of altering cell fates and generating dominant phenotypes. *Development* 118, 401–415.
- S16. Rorth, P. (1998). Gal4 in the *Drosophila* female germline. *Mech. Dev.* 78, 113–118.
- S17. Lee, A., Li, W., Xu, K., Bogert, B.A., Su, K., and Gao, F.B. (2003). Control of dendritic development by the *Drosophila fragile X-related* gene involves the small GTPase Rac1. *Development* 130, 5543–5552.

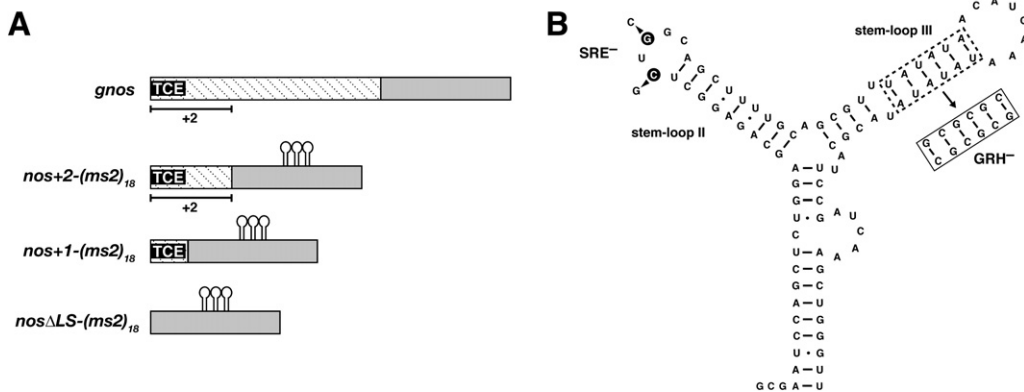


Figure S1. Structure of the *nos* TCE and *nos* Transgenes

(A) The organization of the 3'UTR present within each *nos* transgene is illustrated. Relevant features of the wild-type *nos* 3'UTR (present within the *gnos* transgene) include the previously defined *nos* mRNA localization signal (hatched), with the +2 localization element indicated, and the *nos* TCE (black box), which overlaps but acts independently of the localization signal. The 18 *ms2* binding sites are represented by three stem loops. (B) The *nos* TCE, with stem-loops II and III and the nucleotides altered in *gnosSREs<sup>-</sup>* and *gnosSREs<sup>-</sup>GRH<sup>-</sup>* transgenes indicated.

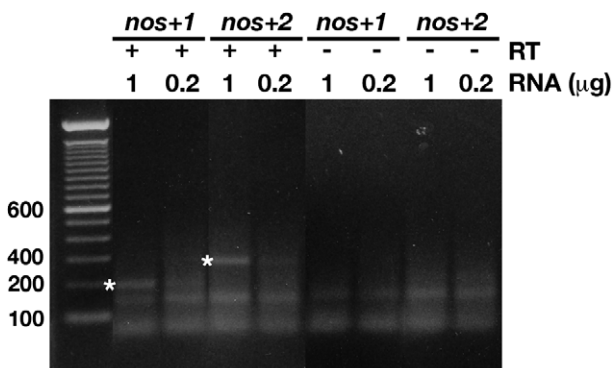


Figure S2. Analysis of *nos+1-(ms2)<sub>18</sub>* and *nos+2-(ms2)<sub>18</sub>* mRNA Levels

RT-PCR analysis of *nos* transgene mRNA levels. For each transgenic line total RNA was isolated from fillet preparations of 30 late third instar larvae by using the QIAGEN RNeasy kit. 0.2  $\mu$ g or 1  $\mu$ g RNA was reverse transcribed by using an oligo dT primer (+RT). Reactions with no reverse transcriptase (-RT) were performed in parallel. 5  $\mu$ l of each reaction was used for PCR amplification with *nos* primers: (5' primer) 5'-CCTGAATTCGCGAATCCAGC TCTG-3' and (3' primer) 5'-CCGCTCGAGTTCGCTTATCTATC-3'. These primers span the *nos* 3'UTR sequences deleted in the transgenic mRNAs, allowing them to be distinguished from the endogenous *nos* transcript. Bands corresponding to the *nos+1-(ms2)<sub>18</sub>* and *nos+2-(ms2)<sub>18</sub>* transcripts are indicated by asterisks. Molecular weight markers are indicated in base pairs.